Coordination, *O*-Methylation, and S−O Bond Cleavage of Sulfur Dioxide on Hexaruthenium Carbido Carbonyl Clusters

Teiji Chihara,*,† Hideaki Kubota,‡ Masashi Fukumoto,§ Haruo Ogawa,‡ Yasuhiro Yamamoto,§ and Yasuo Wakatsuki†

The Institute of Physical and Chemical Research (RIKEN), Wako-shi, Saitama 351-01, Japan, Department of Chemistry, Tokyo Gakugei University, Koganei, Tokyo 184, Japan, and Faculty of Science, Toho University, Funabashi, Chiba 274, Japan

Received April 11, 1997[⊗]

Excess SO_2 gas reacts with the neutral cluster $Ru_6C(CO)_{17}$ (**1**) to substitute only one CO ligand yielding quantitatively $Ru_6C(CO)_{16}(SO_2)$ which reverts to **1** under CO atmosphere. Stepwise substitution of SO_2 for CO in the dianionic cluster $[PPN]_2[Ru_6C(CO)_{16}]$ (PPN = $N\{PPh_3\}_2$) takes place in the presence of trimethylamine oxide to give stable complexes $[PPN]_2[Ru_6C(CO)_{15}(SO_2)]$ (**4**) and $[PPN]_2[Ru_6C(CO)_{14}(SO_2)_2]$. Gaseous NO reacts with **4** to give $[PPN][Ru_6C(CO)_{14}(NO)(SO_2)]$ (**13**), which has not been obtained by the reaction of SO_2 with the NO complex $[PPN][Ru_6C(CO)_{15}(NO)]$ even under forcing conditions. The NO ligand in complex **13** coordinates terminally to a ruthenium atom to which the μ-η^1-SO_2 ligand is bound. The allyl cluster $[PPN][Ru_6C(CO)_{15}(C_3H_5)]$ readily reacts with SO_2 to give $[PPN][Ru_6C(CO)_{14}(C_3H_5)(SO_2)]$ which is also accessible from the reaction of **4** with allyl bromide. Complex **4** readily reacts with an equimolar amount of $MeOSO_2CF_3$ to give $[PPN][Ru_6C(CO)_{15}(SO_2Me)]$ (**7**). On further addition of $MeOSO_2CF_3$ to **7**, or on addition of excess $BF_3{\cdot}OEt_2$ to either **4** or **7**, cleavage of the S−O bond occurs to produce the neutral cluster $Ru_6C(CO)_{15}(SO)$ with a triply bridging SO ligand. The molecular structures of all these new clusters have been characterized by single-crystal X-ray diffraction.

Although a large number of mononuclear and dinuclear complexes with SO_2 ligands have been synthesized and extensively studied,[1−5] there have been relatively few structurally characterized examples of metal cluster complexes containing SO_2 ligand. The majority of SO_2 coordinated clusters are palladium and platinum complexes with[6−8] or without CO ligands.[6,8−19] Only two cobalt subgroup clusters containing sulfur dioxide have been synthesized, *i.e.* $Rh_4(\mu\text{-}CO)_4(\mu\text{-}SO_2)_3[P(OPh)_3]_4$[20] and $Ir_4(CO)_9(\mu\text{-}CO)_2(\mu\text{-}SO_2)$.[21] For the iron triad, several iron[22−24] and osmium clusters[25−27] with SO_2 ligand are known but, to our knowledge, only examples of triruthenium cluster have been reported.[28]

The coordination of a sulfur dioxide molecule to clusters is important as a model for the first step of SO_2 reactions on metal surfaces. In multinuclear clusters, it is of interest which of the available sites the incoming SO_2 will occupy. Successive reactions of cluster-bound SO_2 are likewise of great importance though only a few examples exist. Although not starting from a sulfur dioxide coordinated complex, Kubas and co-workers have isolated the tetranuclear butterfly cluster $Cp_4Mo_4(CO)_2(\mu\text{-}S)_2(\mu\text{-}O)_2$ from the reaction of $Cp_2Mo_2(CO)_6$ with SO_2, a good model for SO_2 reduction by CO on metal surfaces.[1] Shriver and co-workers have synthesized $[HFe_3(CO)_9(SO_2)]^-$ and reduced the coordinated SO_2 with $NaPh_2CO$ to SO or S ligand; for the reduction to sulfido, prior acetylation of SO_2 ligand has been necessary.[23] Methylation of the SO_2 in the same complex by $MeOSO_2CF_3$ has been reported, but no further reaction was suggested.[22] While the most common coordination mode of

† Institute of Physical and Chemical Research.
‡ Tokyo Gakugei University.
§ Toho University.
⊗ Abstract published in *Advance ACS Abstracts,* November 1, 1997.

(1) Kubas, G. J. *Acc. Chem. Res.* **1994**, *27*, 183.
(2) Schenk, W. A. *Angew. Chem., Int. Ed. Eng.* **1987**, *26*, 98.
(3) Vitzthum, G.; Lindner, E. *Angew. Chem., Int. Ed. Engl.* **1971**, *10*, 315.
(4) Wojcicki, A. *Adv. Organomet. Chem.* **1974**, *12*, 31.
(5) Kubas, G. J. *Inorg. Chem.* **1979**, *18*, 182.
(6) Burrows, A. D.; Machell, J. C.; Mingos, D. M. P.; Powell, H. R. *J. Chem. Soc., Dalton Trans.* **1992**, 1521.
(7) Briant, C. E.; Evans, D. G.; Mingos, D. M. P. *J. Chem. Soc., Dalton Trans.* **1986**, 1535.
(8) Mingos, D. M. P.; Wardle, R. W. M. *J. Chem. Soc., Dalton Trans.* **1986**, 73.
(9) Burrows, A. D.; Machell, J. C.; Mingos, D. M. P. *J. Chem. Soc., Dalton Trans.* **1992**, 1939.
(10) Burrows, A. D.; Machell, J. C.; Mingos, D. M. P. *J. Chem. Soc., Dalton Trans.* **1992**, 1991.
(11) Burrows, A. D.; Mingos, D. M. P.; Powell, H. R. *J. Chem. Soc., Dalton Trans.* **1992**, 261.
(12) Burrows, A. D.; Fleisher, H.; Mingos, D. M. P. *J. Organomet. Chem.* **1992**, *433*, 311.
(13) Bott, S. G. O.; Ezomo, J.; Mingos, D. M. P. *J. Chem. Soc., Chem. Commun.* **1988**, 1048.
(14) Otsuka, S.; Tatsuno, Y.; Miki, M.; Aoki, T.; Matsumoto, M.; Yoshioka, H.; Nakatsu, K. *J. Chem. Soc., Chem. Commun.* **1973**, 445.
(15) Mingos, D. M. P.; Williams, I. D.; Watson, M. J. *J. Chem. Soc., Dalton Trans.* **1988**, 1509.
(16) Bott, S. G.; Hallam, M. F.; Ezomo, O. J.; Mingos, D. M. P.; Williams, I. D. *J. Chem. Soc., Dalton Trans.* **1988**, 1461.
(17) Hallam, M. F.; Howells, N. D.; Mingos, D. M. P.; Wardle, R. W. M. *J. Chem. Soc., Dalton Trans.* **1985**, 845.
(18) Evans, D. G.; Hughes, G. R.; Mingos, D. M. P. *J. Chem. Soc., Chem. Commun.* **1980**, 1255.
(19) Moody, D. C.; Ryan, R. R. *Inorg. Chem.* **1977**, *16*, 1052.
(20) Briant, C. E.; Theobald, B. R. C.; Mingos, D. M. P. *J. Chem. Soc., Chem. Commun.* **1981**, 963.
(21) Braga, D.; Ros, R.; Roulet, R. *J. Organomet. Chem.* **1985**, *286*, C8.
(22) Karet, G. B.; Norton, D. M.; Stern, C. L.; Shriver, D. F. *Inorg. Chem.* **1994**, *33*, 5750.
(23) Karet, G. B.; Stern, C. L.; Norton, D. M.; Shriver, D. F. *J. Am. Chem. Soc.* **1993**, *115*, 9979.
(24) Bogdan, P. L.; Sabat, M.; Sunshine, S. A.; Woodcock, C.; Shriver, D. F. *Inorg. Chem.* **1988**, *27*, 1904.
(25) Ewing, P.; Farrugia, L. J. *Organometallics* **1989**, *8*, 1665.
(26) Jarvinen, G. D.; Larson, E. M.; Wasserman, H. J.; Burns, C. J.; Ryan, R. R. *Acta Crystallogr.* **1988**, *C44*, 1701.
(27) Jarvinen G. D.; Ryan, R. R. *Organometallics* **1984**, *3*, 1434.
(28) Karet, G. B.; Stern, L. C.; Cody, J. A.; Lange, S. J.; Pell, M. A.; Slebodnick, C.; Shriver, D. F. *J. Organomet. Chem.* **1995**, *495*, 33.

S0020-1669(97)00429-1 CCC: $14.00

Scheme 1[a]

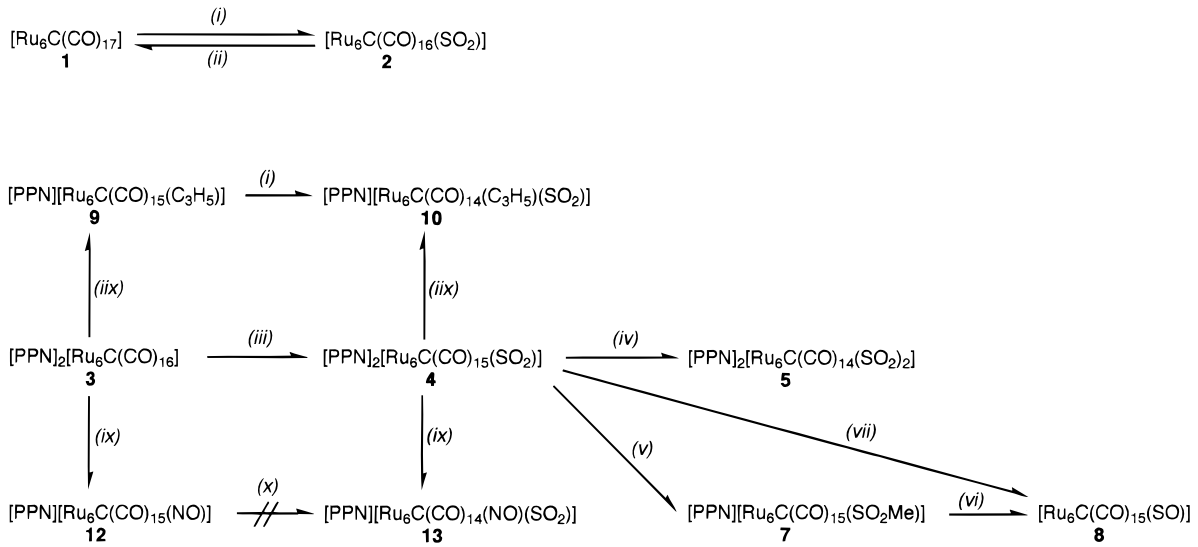

[a] Key: (*i*) SO_2; (*ii*) CO; (*iii*) SO_2 and Me_3NO in MeCN; (*iv*) SO_2 and Me_3NO in MeCN−MeOH; (*v*) $MeOSO_2CF_3$; (*vi*) $BF_3{\cdot}OEt_2$; (*vii*) $MEOSO_2CF_3$ or $BF_3{\cdot}OEt_2$; (*iix*) C_3H_5Br, 85 °C; (*ix*) NO; (*x*) SO_2 and Me_3NO.

SO_2 to clusters is bridging to two metal centers with the S atom, the SO_2 in Shriver's $[HFe_3(CO)_9(SO_2)]^-$ coordinates in μ_3-η^2-fashion donating four electrons; it has not been clear if this unusual binding mode[10,11,20,23] is crucial for the S−O bond cleavage.

Herein we report the syntheses and structural characterizations of several hexaruthenium carbonyl clusters containing sulfur dioxide ligands. Some of the clusters contain NO or organic η^3-C_3H_5 ligands, and the positions of these ligands relative to NO and η^3-C_3H_5 have been determined by X-ray analyses. The SO_2 ligand in the conventional coordination configuration, μ_2-η^1 mode and 2-electron donation, has been found to undergo S−O bond fission by the reaction with $MeOSO_2CF_3$ or BF_3OEt_2 to give a μ_3-SO complex; the reaction occurs with or without prior *O*-methylation of the coordinated SO_2.

The reactions described are summarized in Scheme 1.

Results and Discussion

Reaction of $Ru_6C(CO)_{17}$ (1) with SO_2. Sulfur dioxide was bubbled through a CH_2Cl_2 solution of $Ru_6C(CO)_{17}$ (**1**) and allowed to stand overnight. Treatment by column chromatography gave orange-red crystals in high yield that analyzed correctly for $Ru_6C(CO)_{16}(SO_2)$ (**2**). The same reaction was complete after 1 h when SO_2 was introduced into a refluxing THF solution of **1** or within a few minutes when trimethylamine oxide was added to the SO_2-bubbling solution at ambient temperature. Confirmation of the composition of **2** was obtained by IR and fast atom bombardment mass (FAB mass) spectrometry. Compound **2** showed a mass spectrum with a well defined peak due to $[M]^+$ and exhibited a decomposition pathway with loss of SO_2 and CO ligands. An adduct ion peak $[M - SO_2 + CO]^+$, which corresponds to the parent complex **1**, was also observed. The IR spectra of compound **2** showed the presence of bridging sulfur dioxide ligand: $\nu(SO_2)$ at 1246 and 1076 cm^{-1}. The patterns of the IR spectra in the region for the terminally coordinated CO ligands of **1** and **2** are quite similar, but positions of these peaks in **2** appeared at 2077 s and 2057 vs cm^{-1} which shifted 9 cm^{-1} to higher energy from the corresponding peaks of the parent complex **1** (2068 s and 2048 vs cm^{-1}). This observation indicates that substitution of SO_2 for a CO ligand in this rather large and neutral carbonyl cluster is effective enough to cause withdrawal of some negative charge from the cluster core leading to less effective back-donation to terminal CO's.

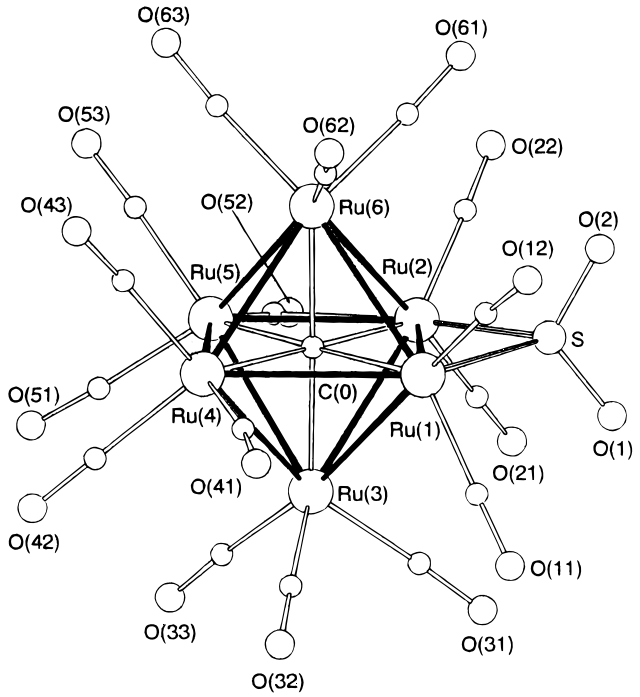

Figure 1. Molecular structure of $Ru_6C(CO)_{17}(SO_2)$ (**2**) with the numbering of the oxygen atoms corresponding to that of the relevant carbonyl carbon atoms. The first digit of each oxygen number is the number of the ruthenium atom to which the carbonyl is attached.

The molecular structure of **2** determined from an X-ray crystallographic analysis is illustrated in Figure 1, and selected intramolecular bond lengths and angles are given in Table 1. The octahedral array of Ru atoms with an interstitial carbide ligand is essentially identical to that of the parent complex **1**.[29] The metal−metal distances in **2** range from 2.8457(6) to 3.0396(6) Å (mean 2.915(17) Å), which are slightly longer than

(29) Braga, D.; Grepioni, F.; Dyson, P. J.; Johnson, B. F. G.; Frediani, P.; Bianchi, M.; Piacenti, F. *J. Chem. Soc., Dalton Trans.* **1992**, 2565. Three isomers are reported in this literature, and these data are calculated from IIA isomer. However, the choice of the isomer dose not affect the result.

Table 1. Selected Bond Lengths (Å) and Angles (deg) for $[Ru_6C(CO)_{16}(SO_2)]$ (**2**)

Ru(1)−Ru(2)	2.8973(9)	Ru(1)−C(0)	2.052(4)
Ru(1)−Ru(3)	2.8568(7)	Ru(2)−C(0)	2.094(4)
Ru(1)−Ru(4)	3.0396(6)	Ru(3)−C(0)	2.051(4)
Ru(2)−Ru(3)	2.9623(8)	Ru(4)−C(0)	2.060(4)
Ru(2)−Ru(5)	2.8457(6)	Ru(5)−C(0)	2.073(4)
Ru(2)−Ru(6)	2.9772(6)	Ru(6)−C(0)	2.035(4)
Ru(1)−Ru(6)	2.8893(6)	S−O(1)	1.437(5)
Ru(3)−Ru(4)	2.8538(6)	S−O(2)	1.452(6)
Ru(3)−Ru(5)	2.9416(7)	Ru(4)−C(41)	1.924(5)
Ru(4)−Ru(5)	2.9189(9)	Ru(1)−C(41)	3.095(5)
Ru(4)−Ru(6)	2.8627(7)	Ru(2)−C(52)	2.619(5)
Ru(5)−Ru(6)	2.9320(7)	Ru(5)−C(52)	1.925(5)
Ru(1)−S	2.284(1)	O(41)−C(41)	1.143(6)
Ru(2)−S	2.327(1)	O(52)−C(52)	1.146(6)
Ru(2)−Ru(1)−S	51.73(3)	Ru(2)−S−O(2)	115.4(2)
Ru(1)−Ru(2)−S	50.41(4)	O(1)−S−O(2)	113.4(3)
S−Ru(2)−C(52)	174.9(1)	Ru(4)−C(41)−O(41)	171.9(5)
Ru(1)−S−Ru(2)	77.9(5)	Ru(2)−C(52)−Ru(5)	75.9(1)
Ru(1)−S−O(1)	116.3(2)	Ru(2)−C(52)−O(52)	120.5(4)
Ru(1)−S−O(2)	115.2(2)	Ru(5)−C(52)−O(52)	163.6(5)
Ru(2)−S−O(1)	114.3(2)		

those of the parent cluster **1** with range from 2.826(1) to 2.998(1) Å (mean 2.893(14) Å). The molecular structure of **2** has an approximate mirror plane defined by Ru(1), Ru(2), Ru(4), Ru(5), and the carbide carbon atom, on which the edge-bridging sulfur dioxide ligand and a semibridging carbonyl ligand are located. All the other CO ligands are coordinated terminally. The S-bridged metal−metal distance (2.8973(9) Å), metal−S distances (2.281(4), 2.327(1) Å), and metal−S−metal angle (77.9(5)°) are all similar to those found in neutral Os complexes $H_2Os_3(CO)_{10}(SO_2)$[27] and $H_2Os_3Pt(CO)_{10}(SO_2)(PCy_3)$;[25] for the similarity of the bonding parameters between ruthenium and osmium carbonyl clusters see ref 30. On the other hand, the S-bridged Ru−Ru distance and Ru−S distances are *ca.* 10% and 5%, respectively, longer than the corresponding values for the neutral iron complexes, $Fe_2Cp_2(CO)_3(SO_2)$[31] and $Fe_2(CO)_7$-(S-*t*-Bu),[32] in accord with the smaller covalent radius of iron.

When a THF solution of **2** was allowed to stand under an atmosphere of CO at ambient temperature for 20 h, it reverted to **1** almost quantitatively; the same reaction at 80 °C in a sealed tube was complete within 1 h. Incomplete substitution of CO ligands for SO_2 ligands has been reported for cationic Pt and Pd clusters: from $[Pt_3Au(SO_2)_3\{P(C_6H_{11})_3\}_4][PF_6]$ to yield $[Pt_3Au(SO_2)(CO)_2\{P(C_6H_{11})_3\}_4][PF_6]$,[8] from $Pd_5(SO_2)_4(PR_3)_5$ (R = Ph or C_6H_4-4-OMe) to $Pd_5(SO_2)_2(CO)_2(PR_3)_5$, and from $Pd_5(SO_2)_4((PMe_2Ph)_5$ to $Pd_5(SO_2)_3(CO)_2(PMe_2Ph)_5$.[6] In some cases a change in cluster nuclearity has been noted, *e.g.* from $Pt_3(SO_2)_3(PPh_3)_3$ to yield $Pd_5(CO)_6(PPh_3)_4$.[7] With the aid of trimethylamine oxide, all the SO_2 ligands were replaced with CO ligands, *i.e.* $Pt_3(SO_2)_3\{P(C_6H_{11})_3\}_3$ gave $Pt_3(CO)_3$-$\{P(C_6H_{11})_3\}_3$.[16] Complete and reversible substitution of SO_2 ligand with CO under very mild conditions as in the present case is rare.

Reaction of $[PPN]_2[Ru_6C(CO)_{16}]$ (3) with SO_2. Addition of trimethylamine oxide to a SO_2-saturated acetonitrile solution of $[PPN]_2[Ru_6C(CO)_{16}]$ (**3**) (PPN = N{PPh_3}$_2$) and subsequent work up gave an air-stable red crystalline solid in reasonable yield which was formulated as $[PPN]_2[Ru_6C(CO)_{15}(SO_2)]$ (**4**) on the basis of analytical data. While the iron version of **4**, $[PPN]_2[Fe_6C(CO)_{15}(SO_2)]$, has been prepared from $[PPN]_2$-$[Fe_6C(CO)_{16}]$ and SO_2 without the aid of trimethylamine oxide,[24] a CH_2Cl_2 solution of **3** saturated with SO_2 gave decomposition products after 1 d when no trimethylamine oxide was added. The IR spectrum of complex **4** in CH_2Cl_2 shows the presence of terminal and bridging carbonyl ligands (2045 w, 1992 vs, 1934 w, 1789 w (br), 1732 w (br) cm^{-1}) as well as bridging sulfur dioxide ligand (1186 m and 1052 s cm^{-1}). However, the spectra of the ν(CO) region is not similar to that reported for the corresponding iron cluster $[PPN]_2[Fe_6C(CO)_{15}(SO_2)]$ (ν(CO), 2040 w, 1982 vs, and 1777 w cm^{-1}; $\nu(SO_2)$, 1180 m and 1045 s cm^{-1} in CH_2Cl_2). For comparison, the parent ruthenium cluster $[Ru_6C(CO)_{16}]^{2-}$ [33] is similar to the corresponding iron cluster $[Fe_6C(CO)_{16}]^{2-}$ [34] in its solid-state structure but differs in the IR spectrum. Since IR spectra are not very helpful in determining the structure, an X-ray crystallographic analysis on **4** was undertaken. The molecular structure of the anion part of **4** is illustrated in Figure 2, while selected interatomic distances and angles are given in Table 2. The octahedral metal skeleton of **4** with an interstitial carbide ligand is essentially identical to that of the parent compound; the average metal−metal distance in **4** is 2.893(9) Å, which is very close to that of $[Me_4N]_2[Ru_6C(CO)_{16}]$ (2.890(8) Å)[33] and $[AsPh_4]_2$-$[Ru_6C(CO)_{16}]$ (2.89 Å).[35] There are two asymmetric (C(45), C(65)) and one highly asymmetric (C(32)) bridging carbonyl ligands as Figure 2 shows, whereas the corresponding iron cluster $[PPN]_2[Fe_6C(CO)_{15}(SO_2)]$ has one symmetrically bridging and two asymmetrically bridging[36] carbonyl ligands, with a corresponding difference in the IR spectra. The SO_2 ligand in **4** bridges the second shortest metal−metal bond, and the bonding parameters of the SO_2 are virtually equal to those in **2**.

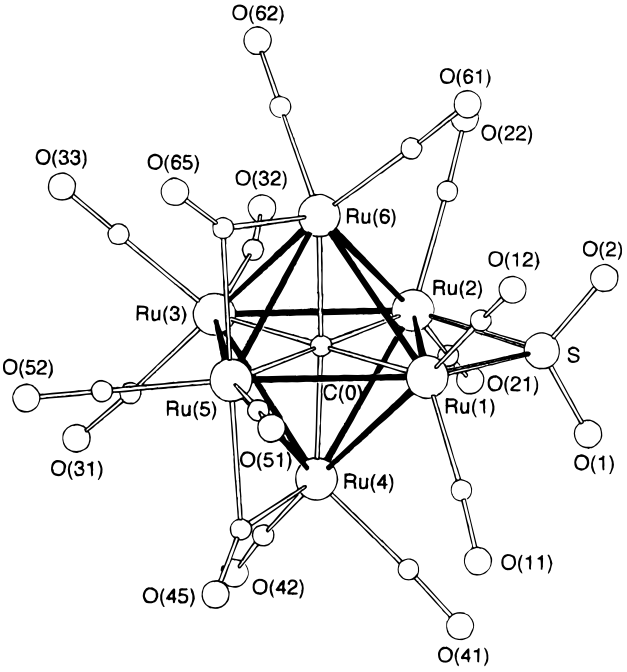

Figure 2. Molecular structure of $[Ru_6C(CO)_{15}(SO_2)]^{2-}$ (anion of **4**) showing the atom-numbering scheme.

Cluster **4** is fairly air-stable in the solid state, and no decomposition was observed after a few months. In sharp

(30) Chihara, T.; Komoto, R.; Kobayashi, K.; Yamazaki, H.; Matsuura, Y. *Inorg. Chem.* **1989**, *28*, 964.
(31) Churchill, M. R.; Kalra, K. L. *Inorg. Chem.* **1973**, *12*, 1650.
(32) Seyferth, D.; Womack, G. B.; Archer, C. M.; Fackler, J. P., Jr., Marler, D. O. *Organometallics* **1989**, *8*, 443.
(33) Ansell, G. B.; Bradley, J. S. *Acta Crystallogr.* **1980**, *B36*, 726.
(34) Churchill, M. R.; Wormald, J. *J. Chem. Soc., Dalton Trans.* **1974**, 2410.
(35) Johnson, B. F. G.; Lewis, J.; Sankey, S. W.; Wong, K.; McPartlin, M.; Nelson, W. J. H. *J. Organomet. Chem.* **1980**, *191*, C3.
(36) Johnson, B. F. G.; Benfield, R. E. *Transition Metal Clusters*; Johnson, B. F. G., Ed.; Wiley: Chichester, U.K., 1980; p 491.

Table 2. Selected Bond Lengths (Å) and Angles (deg) for $[PPN]_2[Ru_6C(CO)_{15}(SO_2)]$ (**4**)

Ru(1)−Ru(2)	2.8581(7)	Ru(3)−C(0)	2.046(5)
Ru(1)−Ru(4)	2.8970(7)	Ru(4)−C(0)	2.047(6)
Ru(1)−Ru(5)	2.9011(7)	Ru(5)−C(0)	2.053(5)
Ru(1)−Ru(6)	2.9217(7)	Ru(6)−C(0)	2.037(6)
Ru(2)−Ru(3)	2.9292(7)	Ru(2)−C(32)	2.862(7)
Ru(2)−Ru(4)	2.9556(7)	Ru(3)−C(32)	1.911(8)
Ru(2)−Ru(6)	2.8916(7)	Ru(4)−C(45)	2.020(6)
Ru(3)−Ru(4)	2.9011(7)	Ru(5)−C(45)	2.268(6)
Ru(3)−Ru(5)	2.8948(7)	Ru(5)−C(65)	2.319(7)
Ru(3)−Ru(6)	2.8450(7)	Ru(6)−C(65)	1.995(6)
Ru(4)−Ru(5)	2.8596(7)	S−O(1)	1.473(5)
Ru(5)−Ru(6)	2.8649(7)	S−O(2)	1.453(6)
Ru(1)−S	2.298(2)	O(32)−C(32)	1.148(10)
Ru(2)−S	2.311(2)	O(45)−C(45)	1.138(8)
Ru(1)−C(0)	2.047(5)	O(65)−C(65)	1.150(8)
Ru(2)−C(0)	2.045(5)		

Ru(2)−Ru(1)−S	51.87(4)	Ru(2)−S−O(2)	116.5(2)
Ru(1)−Ru(2)−S	51.48(4)	O(1)−S−O(2)	113.1(3)
S−Ru(2)−C(32)	176.2(2)	Ru(3)−C(32)−O(32)	169.3(7)
C(45)−Ru(5)−C(65)	178.8(2)	Ru(3)−C(33)−O(33)	179.4(7)
Ru(1)−S−Ru(2)	76.65(5)	Ru(4)−C(45)−O(45)	145.0(5)
Ru(1)−S−O(1)	114.9(2)	Ru(5)−C(45)−O(45)	131.3(5)
Ru(1)−S−O(2)	115.9(2)	Ru(5)−C(65)−O(65)	129.7(5)
Ru(2)−S−O(1)	115.2(2)	Ru(6)−C(65)−O(65)	147.2(6)

contrast to the neutral complex **2**, anionic **4** in THF or CH_2Cl_2 solution remains intact under atmospheric CO pressure even when the reaction temperature is raised to 140 °C in a sealed tube; however, at 180 °C for 1 h, it decomposes to an insoluble material.

Replacement of two CO ligands in **3** by SO_2 by heating in acetonitrile in the presence of a large excess amount of trimethylamine oxide was not possible because of the limited solubility of the oxide. When the same reaction was carried out in an acetonitrile−methanol (1:1 v/v) solution at ambient temperature, the desired reaction took place smoothly to yield the complex $[PPN]_2[Ru_6C(CO)_{14}(SO_2)_2]$ (**5**) without giving any trace amount of **4**. Further substitution was not observed in the same solvent even under more forcing conditions. Starting from SO_2-monosubstituted cluster **4**, the reaction of SO_2 in CH_3CN−MeOH and in the presence of excess trimethylamine oxide stopped again cleanly at the stage of disubstituted complex **5**.

Although the IR spectral pattern of **5** in the carbonyl region is quite similar to those of the starting materials **3** and **4**, the stretching frequency for the terminal CO was observed at 2008 vs cm^{-1}. Therefore, the ν(CO) shifts to higher energy are 15 and 16 cm^{-1} on going from **3** to **4** and further to **5**, indicating a steady decrease of electronic charge in the cluster core by the introduction of SO_2 ligand(s).

In a similar way, a complex with different cation, $[PPh_4]_2[Ru_6C(CO)_{14}(SO_2)_2]$ (**6**), was prepared from $[PPh_4]_2[Ru_6C(CO)_{16}]$ to give good crystals. The structure of the cluster anion of **6** is shown in Figure 3, and selected interatomic distances and angle are listed in Table 3. As Figure 3 shows the two SO_2 ligands are located far apart from each other and bridge the second and the third shortest metal−metal bonds in the cluster. There are two bridging carbonyl ligands. The parent cluster anion in $[AsPh_4]_2[Ru_6C(CO)_{16}]$ has two terminal carbonyl ligands on each ruthenium atom and four edge-bridging carbonyl ligands, giving an approximate overall D_{2d} symmetry.[33] Replacement of two of the bridging carbonyl ligands by bridging SO_2 ligands gives the structure of the anionic part of **6** with approximate C_2 symmetry.

Reaction of $[PPN]_2[Ru_6C(CO)_{15}(SO_2)]$ (4) with $MeOSO_2CF_3$. When a slight excess of methyl trifluoromethanesulfonate ($MeOSO_2CF_3$) was added to a CH_2Cl_2 solution of **4**, the color of the solution changed immediately from red to red-brown. Separation on silica gel column followed by crystallization from CH_2Cl_2−hexane gave deep red-brown crystals with the formula $[PPN][Ru_6C(CO)_{15}(SO_2Me)]$ (**7**). The ^1H NMR spectrum in $CDCl_3$ showed the presence of methoxy group at 3.72 ppm, and the IR spectrum exhibited the presence of two different S−O stretching bands.[22] The molecular structure of the anionic part in **7** is illustrated in Figure 4, and the selected interatomic distances and angles are listed in Table 4.

The methyl cation has attacked one of the SO_2 oxygen atoms to give the monoanionic complex. The metal−sulfur distances are shortened considerably from 2.298(2) and 2.311(2) Å in **4** to 2.228(1) and 2.250(1) Å in **7**, which apparently is the

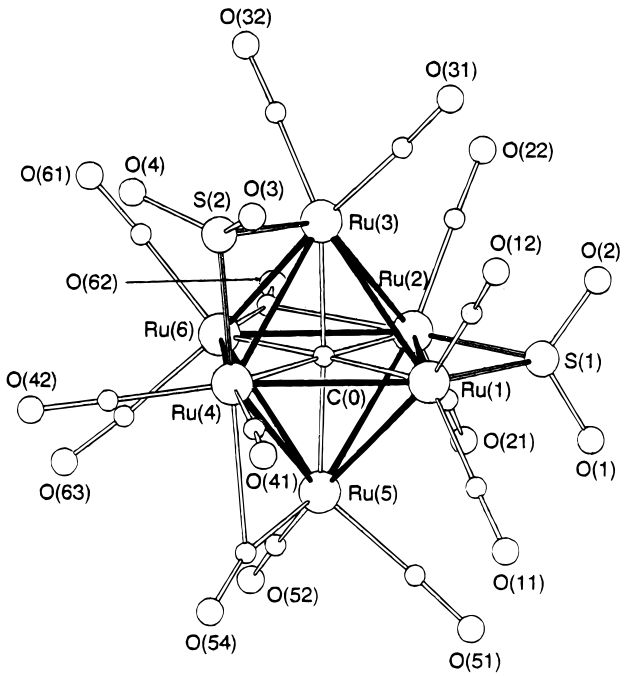

Figure 3. Molecular structure of $[Ru_6C(CO)_{14}(SO_2)_2]^{2-}$ (anion of **6**) showing the atom-numbering scheme.

Table 3. Selected Bond Lengths (Å) and Angles (deg) for $[PPh_4]_2[Ru_6C(CO)_{14}(SO_2)_2]$ (**6**)

Ru(1)−Ru(2)	2.8576(10)	Ru(1)−C(0)	2.029(5)
Ru(1)−Ru(3)	2.9365(9)	Ru(2)−C(0)	2.056(6)
Ru(1)−Ru(4)	2.9507(8)	Ru(3)−C(0)	2.045(6)
Ru(1)−Ru(5)	2.8912(8)	Ru(4)−C(0)	2.050(6)
Ru(2)−Ru(3)	2.9601(13)	Ru(5)−C(0)	2.060(6)
Ru(2)−Ru(5)	2.8933(9)	Ru(6)−C(0)	2.052(5)
Ru(2)−Ru(6)	2.8925(8)	Ru(2)−C(62)	2.656(7)
Ru(3)−Ru(4)	2.8756(9)	Ru(4)−C(54)	2.591(9)
Ru(3)−Ru(6)	2.8940(8)	Ru(5)−C(54)	1.900(8)
Ru(4)−Ru(5)	2.8822(12)	Ru(6)−C(62)	1.905(8)
Ru(4)−Ru(6)	2.8763(10)	S(1)−O(1)	1.451(6)
Ru(5)−Ru(6)	2.8563(9)	S(1)−O(2)	1.439(5)
Ru(1)−S(1)	2.285(2)	S(2)−O(3)	1.443(4)
Ru(2)−S(1)	2.325(2)	S(2)−O(4)	1.463(5)
Ru(3)−S(2)	2.281(2)	O(54)−C(54)	1.169(10)
Ru(4)−S(2)	2.314(2)	O(62)−C(62)	1.152(10)

Ru(2)−Ru(1)−S(1)	52.33(5)	Ru(3)−S(2)−Ru(4)	77.48(6)
Ru(1)−Ru(2)−S(1)	51.07(5)	Ru(3)−S(2)−O(3)	116.4(2)
S(1)−Ru(2)−C(62)	177.9(2)	Ru(3)−S(2)−O(4)	114.6(2)
Ru(4)−Ru(3)−S(2)	51.78(5)	Ru(4)−S(2)−O(3)	116.0(2)
Ru(3)−Ru(4)−S(2)	50.73(4)	Ru(4)−S(2)−O(4)	114.6(2)
S(2)−Ru(4)−C(54)	177.8(2)	O(3)−S(2)−O(4)	113.3(3)
Ru(1)−S(1)−Ru(2)	76.60(5)	Ru(4)−C(54)−Ru(5)	78.2(3)
Ru(1)−S(1)−O(1)	115.0(3)	Ru(4)−C(54)−O(54)	121.7(6)
Ru(1)−S(1)−O(2)	117.2(3)	Ru(5)−C(54)−O(54)	160.1(7)
Ru(2)−S(1)−O(1)	115.4(2)	Ru(2)−C(62)−Ru(6)	76.8(2)
Ru(2)−S(1)−O(2)	115.0(2)	Ru(2)−C(62)−O(62)	121.4(5)
O(1)−S(1)−O(2)	113.0(3)	Ru(6)−C(62)−O(62)	161.8(6)

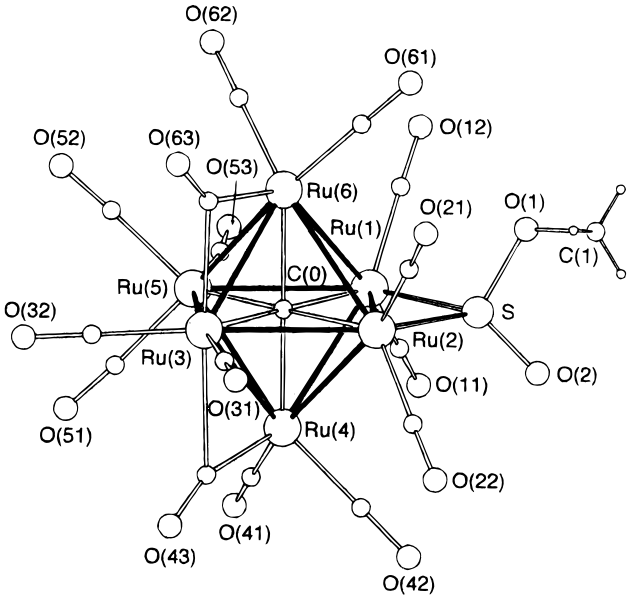

Figure 4. Molecular structure of $[Ru_6C(CO)_{15}(SO_2Me)]^-$ (anion of **7**) showing the atom-numbering scheme.

Table 4. Selected Bond Lengths (Å) and Angles (deg) for [PPN][$Ru_6C(CO)_{15}(SO_2Me)$] (**7**)

Ru(1)−Ru(2)	2.8130(9)	Ru(3)−C(0)	2.024(4)
Ru(1)−Ru(4)	2.8805(13)	Ru(4)−C(0)	2.044(4)
Ru(1)−Ru(5)	2.9595(8)	Ru(5)−C(0)	2.028(4)
Ru(1)−Ru(6)	2.9104(12)	Ru(6)−C(0)	2.049(4)
Ru(2)−Ru(3)	2.8935(7)	Ru(3)−C(43)	2.537(5)
Ru(2)−Ru(4)	2.9023(9)	Ru(4)−C(43)	1.928(5)
Ru(2)−Ru(6)	2.9140(7)	Ru(3)−C(63)	2.218(5)
Ru(3)−Ru(4)	2.9108(12)	Ru(6)−C(63)	2.016(5)
Ru(3)−Ru(5)	2.8827(9)	S−O(1)	1.615(3)
Ru(3)−Ru(6)	2.8635(13)	S−O(2)	1.453(4)
Ru(4)−Ru(5)	2.8733(8)	O(1)−C(1)	1.435(7)
Ru(5)−Ru(6)	2.8754(9)	O(43)−C(43)	1.151(6)
Ru(1)−S	2.228(1)	O(63)−C(63)	1.160(6)
Ru(2)−S	2.250(1)	C(1)−H(1)	0.83(5)
Ru(1)−C(0)	2.060(4)	C(1)−H(2)	0.91(5)
Ru(2)−C(0)	2.056(4)	C(1)−H(3)	0.83(7)

Ru(2)−Ru(1)−S	51.43(3)	Ru(4)−C(43)−O(43)	156.1(4)
Ru(1)−Ru(2)−S	50.74(4)	Ru(3)−C(63)−Ru(6)	85.0(2)
Ru(1)−S−Ru(2)	77.83(4)	Ru(3)−C(63)−O(63)	133.0(4)
Ru(1)−S−O(1)	108.7(1)	Ru(6)−C(63)−O(63)	142.0(4)
Ru(1)−S−O(2)	124.8(1)	C(43)−Ru(3)−C(63)	175.5(2)
Ru(2)−S−O(1)	113.9(1)	O(1)−C(1)−H(1)	106(3)
Ru(2)−S−O(2)	123.3(1)	O(1)−C(1)−H(2)	102(4)
O(1)−S−O(2)	106.1(2)	O(1)−C(1)−H(3)	111(4)
S−O(1)−C(1)	116.9(3)	H(1)−C(1)−H(2)	110(5)
Ru(3)−C(43)−Ru(4)	80.1(2)	H(1)−C(1)−H(3)	112(6)
Ru(3)−C(43)−O(43)	123.8(4)	H(2)−C(1)−H(3)	112(6)

consequence of the change from 2-electron donation of the SO_2 ligand to 3-electron donation of the SO_2Me ligand. The S═O bond distance in **7** remained unchanged while the other S−O is now a single bond (1.615(3) Å). A related neutral iron cluster, $HFe_3(CO)_9(SO_2Me)$, with the μ_3-η^2-SO_2Me ligand has been reported,[22] in which the S−OMe and O−Me separations, 1.603(4) and 1.44(1) Å, are identical to the corresponding values of **7** but S═O separation, 1.511(5) Å, is much larger than in **7** because the nonmethylated O interacts with the Fe_3 cluster.

S−O Bond Cleavage by $MeOSO_2CF_3$ or BF_3·OEt_2. An excess amount of $MeOSO_2CF_3$ reacted with **7** at room temperature. An immediate color change occurred from red-brown to green and eventually a green precipitate formed. Upon recrystallization from CH_2Cl_2−hexane, crystals of the moisture-sensitive neutral cluster $Ru_6C(CO)_{15}(SO)$ (**8**) were obtained in 63% yield. The same complex was directly obtained in

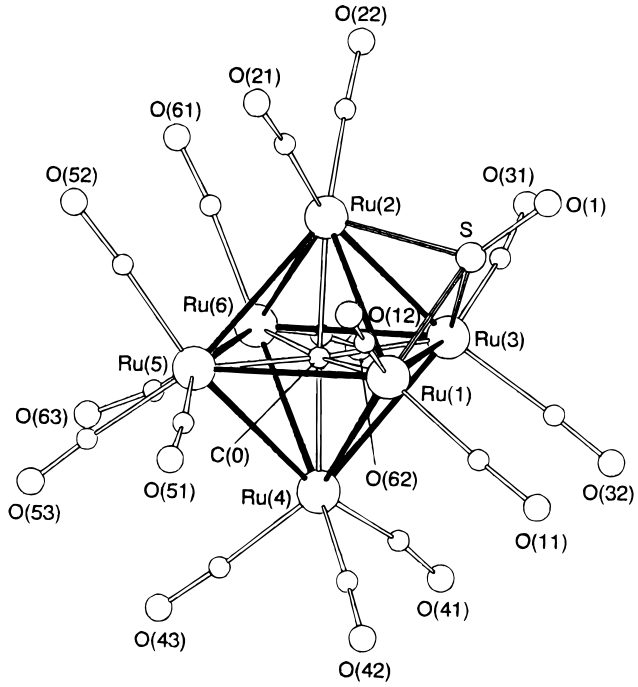

Figure 5. Molecular structure of $Ru_6C(CO)_{15}(SO)$ (**8**) showing the atom-numbering scheme. Crystallographically independent but chemically equivalent clusters are contained in the unit cell, one of which (cluster A) is illustrated. The label "A" for each atom is omitted for clarity.

moderate yield by the reaction of **4** with an excess of $MeOSO_2CF_3$. The IR spectrum of this compound in the S−O stretching region shows only one strong band at 1033 cm^{-1} which is close to the SO stretching vibration reported for the triiron complex [PPN][$Fe_3(CO)_9(SO)$].[23] A single-crystal X-ray analysis has confirmed the cluster formula of $Ru_6C(CO)_{15}(SO)$ (**8**). The unit cell contained two crystallographically unique but essentially identical clusters. A drawing of one of the cluster anions is shown in Figure 5, and the selected interatomic distances and angles are listed in Table 5. The SO ligand triply bridges the three shortest metal−metal bonds and the cluster has an approximate C_3 axis through atoms O(1), S, and C(0). The geometry and dimensions of the metal framework of **8** are almost identical to those of the parent cluster **7** or **4**. Consistent with this coordination mode and satisfying the electron count of 86, the SO ligand works as a 4-electron donor. The metal−sulfur distances, mean 2.238(2) Å, is almost equal to those in **7** in which sulfur donates three electrons to the cluster. However, those separations are shorter than the Ru−S distances in the SO_2 clusters **2**, **4**, and **6** (mean 2.303(7) Å), in which sulfur atom donates two electrons.

In order to examine the fate of the methoxy group in **7**, an aliquot of the supernatant reaction mixture was analyzed carefully by GLC which cleanly indicated the formation of dimethyl ether. The overall reaction then may be expressed as shown in eq 1.

$$\underset{\mathbf{7}}{[PPN][Ru_6C(CO)_{15}(SO_2Me)]} + MeOSO_2BF_3 \rightarrow \underset{\mathbf{8}}{Ru_6C(CO)_{15}(SO)} + MeOMe + [PPN][OSO_2CF_3] \quad (1)$$

The S−O bond cleavage to form **8** was also effected by the reaction of boron trifluoride diethyl etherate (BF_3·OEt_2) with **4** or **7**. On addition of excess BF_3·OEt_2 to a CH_2Cl_2 solution of **7**, the color immediately changed from red-brown to green and deep green crystals of **8** gradually separated. After addition of

Table 5. Selected Bond Lengths (Å) and Angles (deg) for $[Ru_6C(CO)_{15}(SO)]$ (**8**)

cluster A		cluster B	
Ru(1A)−Ru(2A)	2.811(2)	Ru(1B)−Ru(2B)	2.813(2)
Ru(1A)−Ru(3A)	2.827(2)	Ru(1B)−Ru(3B)	2.831(2)
Ru(1A)−Ru(4A)	2.980(2)	Ru(1B)−Ru(4B)	2.961(3)
Ru(1A)−Ru(5A)	2.958(2)	Ru(1B)−Ru(5B)	2.932(2)
Ru(2A)−Ru(3A)	2.814(2)	Ru(2B)−Ru(3B)	2.823(2)
Ru(2A)−Ru(5A)	2.943(2)	Ru(2B)−Ru(5B)	2.963(2)
Ru(2A)−Ru(6A)	2.937(2)	Ru(2B)−Ru(6B)	2.928(3)
Ru(3A)−Ru(4A)	2.935(2)	Ru(3B)−Ru(4B)	2.940(2)
Ru(3A)−Ru(6A)	2.944(2)	Ru(3B)−Ru(6B)	2.977(2)
Ru(4A)−Ru(5A)	2.893(2)	Ru(4B)−Ru(5B)	2.878(2)
Ru(4A)−Ru(6A)	2.882(2)	Ru(4B)−Ru(6B)	2.876(2)
Ru(5A)−Ru(6A)	2.887(2)	Ru(5B)−Ru(6B)	2.880(2)
Ru(1A)−S(A)	2.237(5)	Ru(1B)−S(B)	2.239(4)
Ru(2A)−S(A)	2.245(6)	Ru(2B)−S(B)	2.240(5)
Ru(3A)−S(A)	2.238(6)	Ru(3B)−S(B)	2.231(6)
Ru(1A)−C(0A)	2.08(2)	Ru(1B)−C(0B)	2.02(2)
Ru(2A)−C(0A)	2.10(2)	Ru(2B)−C(0B)	2.04(2)
Ru(3A)−C(0A)	2.06(2)	Ru(3B)−C(0B)	2.11(2)
Ru(4A)−C(0A)	2.00(2)	Ru(4B)−C(0B)	2.05(2)
Ru(5A)−C(0A)	2.04(2)	Ru(5B)−C(0B)	2.01(2)
Ru(6A)−C(0A)	2.04(2)	Ru(6B)−C(0B)	2.08(2)
S(A)−O(1A)	1.46(2)	S(B)−O(1B)	1.52(2)
cluster A		**cluster B**	
Ru(2A)−Ru(1A)−S(A)	51.3(1)	Ru(2B)−Ru(1B)−S(B)	51.1(1)
Ru(3A)−Ru(1A)−S(A)	50.8(1)	Ru(3B)−Ru(1B)−S(B)	50.6(1)
Ru(1A)−Ru(2A)−S(A)	51.0(1)	Ru(1B)−Ru(2B)−S(B)	51.1(1)
Ru(3A)−Ru(2A)−S(A)	51.0(1)	Ru(3B)−Ru(2B)−S(B)	50.7(1)
Ru(1A)−Ru(3A)−S(A)	50.8(1)	Ru(1B)−Ru(3B)−S(B)	50.8(1)
Ru(2A)−Ru(3A)−S(A)	51.2(1)	Ru(2B)−Ru(3B)−S(B)	51.0(1)
Ru(1A)−S(A)−Ru(2A)	77.7(2)	Ru(1B)−S(B)−Ru(2B)	77.8(1)
Ru(1A)−S(A)−Ru(3A)	78.4(2)	Ru(1B)−S(B)−Ru(3B)	78.6(2)
Ru(2A)−S(A)−Ru(3A)	77.8(2)	Ru(2B)−S(B)−Ru(3B)	78.3(2)
Ru(1A)−S(A)−O(1A)	135.4(8)	Ru(1B)−S(B)−O(1B)	135.0(7)
Ru(2A)−S(A)−O(1A)	131.4(7)	Ru(2B)−S(B)−O(1B)	132.7(7)
Ru(3A)−S(A)−O(1A)	133.4(7)	Ru(3B)−S(B)−O(1B)	132.0(7)

water to the reaction mixture in order to hydrolyze BF_3-related compounds, both aqueous and CH_2Cl_2 solutions were analyzed by GLC. Methanol was detected in the aqueous solution. Formation of **8** and methanol may be explained as in eqs 2 and 3.

$$[PPN][Ru_6C(CO)_{15}(SO_2Me)] + BF_3 \rightarrow \underset{\mathbf{7}}{} \quad Ru_6C(CO)_{15}(SO) + [PPN][MeOBF_3] \quad (2)$$
$$\mathbf{8}$$

$$[PPN][MeOBF_3] + H_2O \rightarrow [PPN][HOBF_3] + MeOH \quad (3)$$

The formation of **8** by the direct reaction of **4** with BF_3OEt_2 is formally the result of $[O]^{2-}$ removal from the SO_2 ligand. Adduct formation between organic tetrahydrothiophene 1,1-dioxide, $(CH_2)_4SO_2$, and gaseous BF_3 has been known,[37] which dissociates back to the dioxide and BF_3 on heating to 37 °C. On the cluster frame, however, the S−O bond of the present μ_2-coordinated SO_2 ligand was cleaved under mild condition probably forming a boron oxide.

Since free SO is an unstable molecule, which disproportionates rapidly to S or S_2O and SO_2,[38] the number of the examples of SO metal complexes is limited. Three cluster complexes with SO ligand have been reported, two of which have been synthesized by oxidation of a sulfido ligand.[39−43] Only one example of reduction of coordinated SO_2 ligand in a cluster complex has been reported by Shriver and co-workers, *i.e.* reduction of $[PPN][HFe_3(CO)_9(\mu_3\text{-}SO_2)]$ with $NaPh_2CO$ to give $[PPN]_2[Fe_3(CO)_9(\mu_3\text{-}SO)]$ with concomitant loss of the hydride.[23]

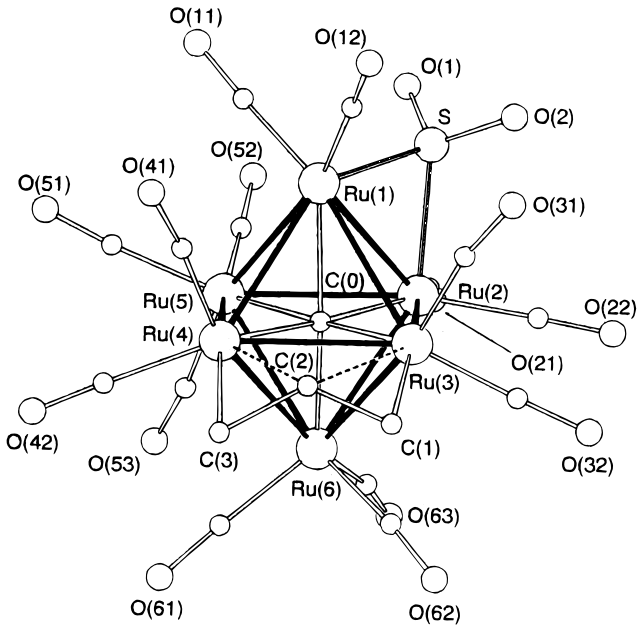

Figure 6. Molecular structure of $[Ru_6C(CO)_{14}((C_3H_5)(SO_2)]^-$ (anion of **11**) showing the atom-numbering scheme. Crystallographically independent but chemically equivalent clusters are contained in the unit cell, one of which (cluster A) is illustrated. The label "A" for each atom is omitted for clarity.

Reaction of [PPN][$Ru_6C(CO)_{15}(C_3H_5)$] (9) with SO_2. In contrast to the reaction of **3** with SO_2, a monoanionic cluster having a μ_2-η^3-allyl ligand, $[PPN][Ru_6C(CO)_{15}(C_3H_5)]$ (**9**), underwent rapid reaction with SO_2. Thus on bubbling SO_2 through a solution of **9** in CH_2Cl_2 at room temperature, the color immediately changed from red to red-brown. Subsequent work up by column chromatography gave red-brown crystalline solid analyzing as $[PPN][Ru_6C(CO)_{14}(C_3H_5)(SO_2)]$ (**10**). The IR and ^1H NMR data, and elemental analyses are consistent with the presence of both allyl and SO_2 ligands. The reaction of the methyl cluster $[PPN][Ru_6C(CO)_{16}Me]$ with SO_2 also proceeded very smoothly at room temperature in the absence of trimethylamine oxide although the product was too unstable to be isolated.

The structural determination of **10** by single-crystal X-ray diffraction was hampered by a serious disorder problem, so the [PPN] cation was replaced with $[PPh_4]$ by starting from $[PPh_4]$-$[Ru_6C(CO)_{15}(C_3H_5)]$ to obtain $[PPh_4][Ru_6C(CO)_{14}(C_3H_5)(SO_2)]$ (**11**). The unit cell of **11** contains two crystallographically unique but essentially identical cluster units. A drawing of one of them is shown in Figure 6, and the selected interatomic distances and angles are listed in Table 6. The SO_2 ligand bridges one of the edges in a usual μ_2-fashion, while the allyl group bridges another edge away from SO_2, retaining its original μ_2-η^3-coordination mode. The bonding parameters of both SO_2 and allyl ligands are identical to those of **4** and **9**, respectively.

Complex **10** could be obtained by another route: A CH_2Cl_2 solution of **4** and allyl bromide was heated at 85 °C for 1 h in

(37) Jones, J. G. *Inorg. Chem.* **1966**, *5*, 1229.
(38) Herron, J. T.; Huie, R. E. *Chem. Phys. Lett.* **1980**, *76*, 322.
(39) Lorenz, I.-P.; Messelhäuser, J. *Z. Naturforsch.* **1984**, *39b*, 403.
(40) Hoots, J. E.; Lesch, D. A.; Rauchfuss, T. B. *Inorg. Chem.* **1984**, *23*, 3130.
(41) Winter, A.; Zsolnai, L.; Huttner, G. *J. Organomet. Chem.* **1982**, *234*, 337.
(42) Markó, L.; Markó-Monostory B.; Madach, T.; Vahrenkamp, H. *Angew. Chem., Int. Ed. Engl.* **1980**, *19*, 226.
(43) Müller, A.; Krickemeyer, E.; Jostes, R.; Bögge, H.; Diemann, E.; Bergmann, U. *Z. Naturforsch.* **1985**, *40b*, 1715.

Table 6. Selected Bond Lengths (Å) and Angles (deg) for $[PPh_4][Ru_6C(CO)_{14}(C_3H_5)(SO_2)]$ (**11**)

cluster A		cluster B	
Ru(1A)−Ru(2A)	2.888(2)	Ru(1B)−Ru(2B)	2.868(2)
Ru(1A)−Ru(3A)	2.963(2)	Ru(1B)−Ru(3B)	2.968(2)
Ru(1A)−Ru(4A)	2.944(2)	Ru(1B)−Ru(4B)	2.910(2)
Ru(1A)−Ru(5A)	2.871(2)	Ru(1B)−Ru(5B)	2.867(2)
Ru(2A)−Ru(3A)	2.887(2)	Ru(2B)−Ru(3B)	2.886(2)
Ru(2A)−Ru(5A)	2.929(2)	Ru(2B)−Ru(5B)	2.978(2)
Ru(2A)−Ru(6A)	2.877(2)	Ru(2B)−Ru(6B)	2.920(2)
Ru(3A)−Ru(4A)	2.898(2)	Ru(3B)−Ru(4B)	2.901(2)
Ru(3A)−Ru(6A)	2.904(2)	Ru(3B)−Ru(6B)	2.918(2)
Ru(4A)−Ru(5A)	2.849(2)	Ru(4B)−Ru(5B)	2.837(2)
Ru(4A)−Ru(6A)	2.898(2)	Ru(4B)−Ru(6B)	2.897(2)
Ru(5A)−Ru(6A)	2.853(2)	Ru(5B)−Ru(6B)	2.866(2)
Ru(1A)−S(A)	2.296(5)	Ru(1B)−S(B)	2.296(5)
Ru(2A)−S(A)	2.303(5)	Ru(2B)−S(B)	2.300(5)
Ru(1A)−C(0A)	2.11(2)	Ru(1B)−C(0B)	2.05(2)
Ru(2A)−C(0A)	2.08(2)	Ru(2B)−C(0B)	2.08(2)
Ru(3A)−C(0A)	1.98(2)	Ru(3B)−C(0B)	2.02(2)
Ru(4A)−C(0A)	2.01(2)	Ru(4B)−C(0B)	2.02(2)
Ru(5A)−C(0A)	2.10(2)	Ru(5B)−C(0B)	2.09(2)
Ru(6A)−C(0A)	2.01(2)	Ru(6B)−C(0B)	2.05(2)
Ru(3A)−C(1A)	2.19(2)	Ru(3B)−C(1B)	2.18(2)
Ru(3A)−C(2A)	2.62(2)	Ru(3B)−C(2B)	2.67(2)
Ru(4A)−C(2A)	2.56(2)	Ru(4B)−C(2B)	2.53(2)
Ru(4A)−C(3A)	2.28(1)	Ru(4B)−C(3B)	2.19(2)
S(A)−O(1A)	1.477(12)	S(B)−O(1B)	1.474(14)
S(A)−O(2A)	1.481(13)	S(B)−O(2B)	1.492(13)
C(1A)−C(2A)	1.41(3)	C(1B)−C(2B)	1.48(3)
C(2A)−C(3A)	1.53(3)	C(2B)−C(3B)	1.49(3)
cluster A		**cluster B**	
Ru(2A)−Ru(1A)−S(A)	51.2(1)	Ru(2B)−Ru(1B)−S(B)	51.5(1)
Ru(1A)−Ru(2A)−S(A)	51.0(1)	Ru(1B)−Ru(2B)−S(B)	51.3(1)
Ru(4A)−Ru(3A)−C(1A)	83.9(5)	Ru(4B)−Ru(3B)−C(1B)	83.0(6)
Ru(4A)−Ru(3A)−C(2A)	54.9(5)	Ru(4B)−Ru(3B)−C(2B)	53.7(5)
C(1A)−Ru(3A)−C(2A)	32.6(7)	C(1B)−Ru(3B)−C(2B)	33.6(8)
C(1A)−Ru(3A)−C(3A)	45.2(6)	C(1B)−Ru(3B)−C(3B)	45.6(7)
Ru(3A)−Ru(4A)−C(2A)	57.1(5)	Ru(3B)−Ru(4B)−C(2B)	58.5(5)
Ru(3A)−Ru(4A)−C(3A)	88.4(6)	Ru(3B)−Ru(4B)−C(3B)	89.0(6)
C(1A)−Ru(4A)−C(3A)	49.3(7)	C(1B)−Ru(4B)−C(3B)	49.6(7)
C(2A)−Ru(4A)−C(3A)	36.3(7)	C(2B)−Ru(4B)−C(3B)	36.0(8)
Ru(1A)−S(A)−Ru(2A)	77.8(2)	Ru(1B)−S(B)−Ru(2B)	77.2(2)
Ru(1A)−S(A)−O(1A)	116.5(6)	Ru(1B)−S(B)−O(1B)	115.8(6)
Ru(1A)−S(A)−O(2A)	113.6(5)	Ru(1B)−S(B)−O(2B)	113.3(5)
Ru(2A)−S(A)−O(1A)	116.2(5)	Ru(2B)−S(B)−O(1B)	116.0(5)
Ru(2A)−S(A)−O(2A)	115.0(6)	Ru(2B)−S(B)−O(2B)	116.6(6)
O(1A)−S(A)−O(2A)	113.3(8)	O(1B)−S(B)−O(2B)	113.3(8)
Ru(3A)−C(1A)−C(2A)	91.0(12)	Ru(3B)−C(1B)−C(2B)	91.7(13)
Ru(3A)−C(2A)−Ru(4A)	68.0(4)	Ru(3B)−C(2B)−Ru(4B)	67.8(4)
Ru(3A)−C(2A)−C(1A)	56.4(11)	Ru(3B)−C(2B)−C(1B)	54.7(10)
Ru(3A)−C(2A)−C(3A)	119.9(10)	Ru(3B)−C(2B)−C(3B)	116.7(12)
Ru(4A)−C(2A)−C(1A)	117.2(12)	Ru(4B)−C(2B)−C(1B)	114.1(11)
Ru(4A)−C(2A)−C(3A)	61.9(8)	Ru(4B)−C(2B)−C(3B)	59.4(12)
C(1A)−C(2A)−C(3A)	124.8(18)	C(1B)−C(2B)−C(3B)	121.7(20)
Ru(4A)−C(3A)−C(2A)	81.8(9)	Ru(4B)−C(3B)−C(2B)	84.6(13)

a pressure bottle. Workup of the resulting solution by silica gel chromatography afforded crystals of **10** in 20% yield. The variable-temperature NMR spectrum of **10** has previously been reported, which shows dynamics of this cluster in solution brought about by CO and SO_2 scrambling on the hexaruthenium core.[44]

Reaction of $[PPN]_2[Ru_6C(CO)_{15}(SO_2)]$ (4) with NO. Previously, we have examined in detail the reaction of gaseous NO with ruthenium carbide clusters including those of **3** and **9**.[45] We were interested to know whether SO_2 and NO could be trapped in a same cluster complex. Only one cluster complex

(44) Chihara, T.; Jesorka, A.; Ikezawa, H.; Wakatsuki, Y. *J. Chem. Soc., Dalton Trans.* **1997**, 443.

(45) Chihara, T.; Sawamura, K.; Ikezawa, H.; Ogawa, H.; Wakatsuki, Y. *Organometallics* **1996**, *15*, 415.

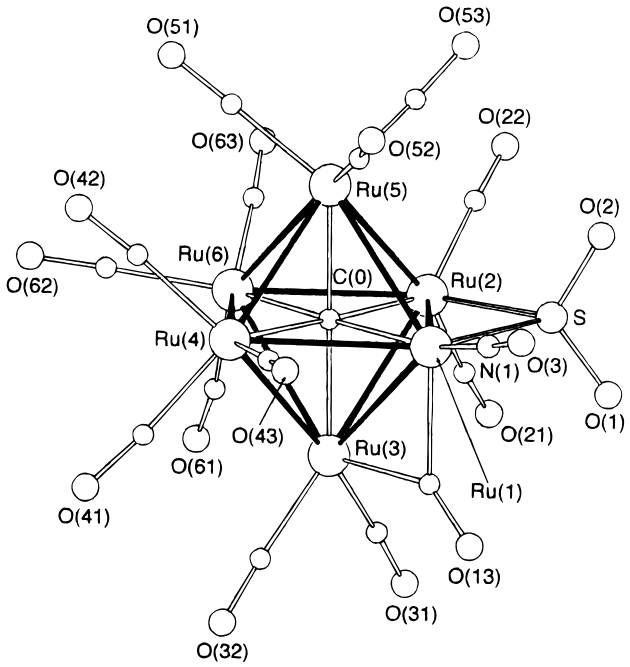

Figure 7. Molecular structure of $[Ru_6C(CO)_{14}(NO)(SO_2)]^-$ (anion of **13**) showing the atom-numbering scheme.

bearing both NO and SO_2 ligands has been reported, *i.e.* $Pd_3(\mu\text{-NO})(\mu\text{-SO}_2)(\mu\text{-Cl})(PPh_3)_3$, and this was synthesized by the substitution of $[NO]^+$ for one of the SO_2 ligands in $[Pd_3(\mu\text{-SO}_2)_2(\mu\text{-Cl})(PPh_3)_3]^-$.[9] However, structural characterization of this compound was not carried out so the relative position of the ligands was not clear.

When gaseous NO was bubbled through a CH_2Cl_2 solution of $[PPN]_2[Ru_6C(CO)_{15}(SO_2)]$ (**4**), only a small color change was noted and so the reaction was monitored by IR spectroscopy. After chromatographic purification of the reaction mixture, a red crystalline solid $[PPN][Ru_6C(CO)_{14}(NO)(SO_2)]$ (**13**) was obtained. The IR spectra of this compound showed the presence of the SO_2 ligand (1231 m and 1068 s cm^{-1}), while the ν(CO) band shifted *ca.* 40 cm^{-1} to higher energy from **4** indicating that the negative charge on the cluster had changed from −2. The reduction of negative charge was what we had expected because gaseous NO, a three electron donor, reacted with the dianionic carbonyl cluster **3** to give the corresponding monoanionic nitrosyl cluster $[PPN][Ru_6C(CO)_{15}(NO)]$ (**12**) in a high yield.[45]

The structure of **13** was confirmed by an X-ray single-crystal analysis to be that of expected as $[PPN][Ru_6C(CO)_{14}(SO_2)(NO)]$. The NO ligand has been assigned by *ca.* 0.14 Å shorter Ru−N(=O) separation as compared to the Ru−C(=O) values. The molecular structure of the cluster anion in **13** is shown in Figure 7, while the selected interatomic distances and angles are listed in Table 7. Interestingly, the terminally coordinating NO ligand is on the metal atom to which the SO_2 ligand coordinates in a μ_2-fashion.

Surprisingly, an attempt to prepare **13** by the reaction of **12** with gaseous SO_2 was not successful. Bubbling of gaseous SO_2 into a CH_2Cl_2, methanol, or acetonitrile solution of **12** caused no appreciable reaction even with prolonged reaction time at room temperature or under reflux. Moreover, addition of trimethylamine oxide to the solution had no effect on the reaction, the starting material **12** having been recovered quantitatively.

Conclusion

A series of neutral, monoanionic, and dianionic hexaruthenium carbido carbonyl clusters with SO_2 ligand(s) have been

Table 7. Selected Bond Lengths (Å) and Angles (deg) for [PPN][$Ru_6C(CO)_{15}(NO)(SO_2)$] (**13**)

Ru(1)−Ru(2)	2.8745(8)	Ru(1)−C(O)	2.076(4)
Ru(1)−Ru(3)	2.8310(8)	Ru(2)−C(O)	2.049(4)
Ru(1)−Ru(4)	2.9849(10)	Ru(3)−C(O)	2.055(4)
Ru(1)−Ru(5)	2.9175(9)	Ru(4)−C(O)	2.055(4)
Ru(2)−Ru(3)	2.9438(8)	Ru(5)−C(O)	2.046(4)
Ru(2)−Ru(5)	2.9324(8)	Ru(6)−C(O)	2.024(3)
Ru(2)−Ru(6)	2.8898(9)	Ru(1)−N(1)	1.760(4)
Ru(3)−Ru(4)	2.8934(8)	Ru(1)−C(13)	2.073(5)
Ru(3)−Ru(6)	2.9846(9)	Ru(3)−C(13)	2.046(5)
Ru(4)−Ru(5)	2.8330(8)	S−O(1)	1.454(3)
Ru(4)−Ru(6)	2.8511(8)	S−O(2)	1.455(4)
Ru(5)−Ru(6)	2.8629(8)	O(3)−N(1)	1.164(6)
Ru(1)−S	2.3201(14)	O(13)−C(13)	1.165(6)
Ru(2)−S	2.2853(12)		
Ru(2)−Ru(1)−S	50.84(3)	Ru(2)−S−O(1)	117.0(1)
Ru(1)−Ru(2)−S	51.92(4)	Ru(2)−S−O(2)	116.1(1)
S−Ru(1)−N(1)	100.0(1)	O(1)−S−O(2)	113.9(2)
S−Ru(1)−C(13)	93.4(1)	Ru(1)−N(1)−O(3)	175.0(4)
N(1)−Ru(1)−C(13)	101.3(2)	Ru(1)−C(13)−Ru(3)	86.8(2)
Ru(1))−S−Ru(2)	77.24(4)	Ru(1)−C(13)−O(13)	133.8(4)
Ru(1)−S−O(1)	114.8(2)	Ru(3)−C(13)−O(13)	139.4(4)
Ru(1)−S−O(2)	112.6(2)		

synthesized by SO_2 replacement of coordinated CO. In the case of [PPN][$Ru_6C(CO)_{14}(NO)(SO_2)$] (**13**), however, the complex was accessible only from the complex [PPN]$_2$[$Ru_6C(CO)_{15}(SO_2)$] (**4**) and gaseous NO. The SO_2 ligand is bound to the cluster only weakly in the case of neutral cluster, $Ru_6C(CO)_{16}(SO_2)$ (**2**); thus, the SO_2 is replaced by CO at atmospheric pressure. Sulfur dioxide is more strongly bonded to anionic clusters. Apparently this tendency is related to strongly electron-withdrawing character of the SO_2 ligand, which is evidenced by shifts of the IR ν(C═O) bands to higher energy on introduction of the SO_2 ligand. The organic electrophile CH_3^+ and the Lewis acid BF_3 produced rapid removal of oxygen from SO_2 bound to the anionic cluster **4** in the conventional μ_2-η^1-fashion to give a neutral cluster with μ_3-η^1-SO.

Experimental Section

The complexes $Ru_6C(CO)_{17}$ (**1**),[46] [PPN]$_2$[$Ru_6C(CO)_{16}$] (**3**),[47] [PPN][$Ru_6C(CO)_{15}(C_3H_5)$] (**9**), [PPN][$Ru_6C(CO)_{16}Me$],[48] and [PPN][$Ru_6C(CO)_{15}(NO)$] (**13**)[45] were synthesized according to literature methods. Methyl trifluoromethanesulfonate, boron trifluoride ether complex, trimethylamine *N*-oxide dihydrate, and sulfur dioxide were commercially available and used as received. Solvents used for reaction were dried and stored over zeolite 4A under argon. All the reactions were carried out under argon. IR and ^{1}H NMR spectra were recorded on a Perkin-Elmer 1600 spectrophotometer and a JEOL RX-270 spectrometer. FAB-MS spectra were obtained with a JEOL JMS-HX 110A double-focusing spectrometer using *m*-nitrobenzyl alcohol as a liquid matrix. GLC measurements were carried out by a Shimadzu GC-7 gas chromatography on a column of Chromosorb 101, 25 wt % sebaconitrile on Uniport C, and 5 wt % bis(2,3-dihydroxypropyl) ether on Chromosorb WAW DMCS.

Synthesis of $Ru_6C(CO)_{16}(SO_2)$ (2). Through a solution of **1** (0.203 g, 0.185 mmol) in CH_2Cl_2 (100 cm^3) in a 300 cm^3 flask SO_2 was bubbled (three bubble/s) for 15 min and allowed to stand for 20 h at ambient temperature. After removal of the solvent from the reaction mixture under reduced pressure the residue was taken up in CH_2Cl_2 and chromatographed on a cellulose column (1.8 cm internal diameter × 25 cm). Elution with hexane separated a red band which was unreacted **1** (23 mg). The second red band was eluted with CH_2Cl_2. Evaporation of the eluate to dryness followed by recrystallization from hot THF gave a red solid (185 mg, 85% based on reacted **1**) (Found: C, 18.40. Calcd for $C_{17}O_{18}Ru_6S$: C, 18.06). IR (cm^{-1}): ν(CO) (CH_2Cl_2) 2108 w, 2077 s, 2057 vs, and 2013 w; ν(SO) (KBr) 1246 m, 1076 s. FAB mass spectrum: *m/z* 1132 ([M]$^+$, 87), 1096 ([M − SO_2 + CO]$^+$, 49), 1068 ([M − SO_2]$^+$, 100), 1040 ([M − SO_2 − CO]$^+$, 51), and 1012 ([M − SO_2 − 2CO]$^+$, 27%).

Reaction of $Ru_6C(CO)_{16}(SO_2)$ (2) with CO. Complex **2** (25 mg, 0.022 mmol) was dissolved in THF (15 cm^3) in a 100 cm^3 flask under CO atmosphere and allowed to stand for 20 h at ambient temperature. After removal of the solvent from the reaction mixture under reduced pressure the residue was taken up in CH_2Cl_2 and chromatographed on a cellulose column (1.8 cm internal diameter × 25 cm). Elution with hexane produced a red band, which was collected and evaporated to dryness followed by recrystallization from CH_2Cl_2−hexane giving dark red crystals of **1** (18 mg, 77%). IR (cm^{-1}): ν(CO) (CH_2Cl_2) 2102 w, 2068 s, 2048 vs, and 2005 w cm^{-1}.

Synthesis of [PPN]$_2$[$Ru_6C(CO)_{15}(SO_2)$] (4). Through a solution of **3** (0.500 g, 0.233 mmol) in acetonitrile (5 cm^3) SO_2 was bubbled for 5 min and trimethylamine oxide dihydrate (0.065 g, 0.583 mmol) was added with stirring, giving a color change from red to orange-red without delay. Immediately the solution was filtered through a short alumina column (1.8 cm internal diameter × 10 cm) using THF as an eluate followed by evaporation of the solvent to dryness. The resulted solid was worked up by alumina column chromatography (5% water, 1.8 cm internal diameter × 20 cm). The red band eluted with THF was collected and evaporated to dryness. Recrystallization of the residue from CH_2Cl_2−ethanol gave red crystals (0.316 g, 62%) (Found: C, 48.57; H, 2.97; N, 1.29. Calcd for $C_{88}H_{60}N_2O_{17}P_4Ru_6S$: C, 48.49; H, 2.77; N, 1.29.). IR (cm^{-1}): ν(CO) (CH_2Cl_2) 2045 w, 1992 vs, 1934 w, 1789 w (br), and 1732 w (br); ν(SO) (KBr) 1186 m and 1052 s cm^{-1}.

Synthesis of [PPN]$_2$[$Ru_6C(CO)_{14}(SO_2)_2$] (5). Through a solution of **3** (0.500 g, 0.233 mmol) in acetonitrile−methanol (10 cm^3/10 cm^3) SO_2 was bubbled for 5 min and trimethylamine oxide (0.052 g, 0.47 mmol) was added with stirring, giving an instant but slight lightening of the color. The solvent was immediately removed under reduced pressure, the residue was taken up in CH_2Cl_2, and the solution was chromatographed on silica gel (3% water, 1.8 cm internal diameter × 20 cm). Elution with CH_2Cl_2-THF (4:1 v/v) produced a red band which was collected. Evaporation of the eluate to dryness followed by recrystallization from ethanol−hexane gave a red solid (0.233 mg, 45%) (Found: C, 47.00 H, 2.88; N, 1.30. Calcd for $C_{87}H_{60}N_2O_{18}P_4Ru_6S$: C, 41.16; H, 2.73; N, 1.26.). IR (cm^{-1}): ν(CO) (CH_2Cl_2) 2053 w, 2008 vs; ν(SO) (KBr) 1055s cm^{-1}.

In an analogous manner, reaction of complex **4** (100 mg, 0.046 mmol) with SO_2 and trimethylamine oxide (5.1 mg, 0.046 mmol) in acetonitrile−methanol (2 cm^3/2 cm^3) solution yielded the title complex (61 mg, 60%).

Synthesis of [PPN][$Ru_6C(CO)_{15}(SO_2Me)$] (7). To a CH_2Cl_2 (3 cm^3) solution of **4** (100 mg, 0.046 mmol) was slowly added $MeOSO_2CF_3$ (20 μL, 0.088 mmol) under vigorous stirring until no starting material could be detected by IR or TLC on silica gel. The color changed from red to red-brown. The solution was worked up by silica gel column chromatography (3% water, 1.8 cm internal diameter × 20 cm). Elution with CH_2Cl_2 separated an orange band. Evaporation of the solvent followed by recrystallization from CH_2Cl_2−methanol afforded red-brown crystals (53 mg, 70%) (Found: C, 38.26; H, 2.03; N, 0.77. Calcd for $C_{53}H_{33}NO_{17}P_2Ru_6S$: C, 38.43; H, 2.01; N, 0.85%). IR (cm^{-1}): ν(CO) (CH_2Cl_2) 2063 w, 2021 sh, 2010 vs, 1956 w (br), and 1811 w; ν(SO) (KBr) 1148 m and 955 s. ^{1}H NMR ($CDCl_3$): 3.72 (3H, s, Me), 7.38−7.63 (30H, m, C_6H_5).

Synthesis of $Ru_6C(CO)_{15}(SO)$ (8). To a CH_2Cl_2 (2 cm^3) solution of **7** (50 mg, 0.030 mmol) was added BF_3·OEt_2 (25 μL, 0.22 mmol) at once with stirring. The color changed immediately from red-brown to green. After removal of the solvent the remaining solid was washed with ether (5 × 2 cm^3). Recrystallization of the product from CH_2Cl_2−hexane gave deep green crystals (21 mg, 65%) (Found: C, 17.69. Calcd for $C_{16}O_{16}Ru_6S$: C, 17.69). IR(cm^{-1}): ν(CO) (CH_2Cl_2) 2098 w, 2052 vs, 2033 w, 2003 w; ν(SO) (KBr) 1033 s cm^{-1}.

Synthesis of [PPN][$Ru_6C(CO)_{14}(C_3H_5)(SO_2)$] (10). Sulfur dioxide was bubbled through a solution of **9** (100 mg, 0.062 mmol) in CH_2Cl_2 (5 cm^3) for 10 min. The solvent was removed from the resulting solution under reduced pressure, and the resulting solid was worked

(46) Nicholls, J. N.; Vargas, M. D. *Inorg. Synth.* **1989**, *26*, 280.
(47) Hayward, C. T.; Shapley, J. R. *Inorg. Chem.* **1982**, *21*, 3816.
(48) Chihara, T.; Aoki, K.; Yamazaki, H. *J. Organomet. Chem.* **1990**, *383*, 367.

Table 8. Crystallographic Data for $Ru_6C(CO)_{16}(SO_2)$ (**2**), $[PPN]_2[Ru_6C(CO)_{15}(SO_2)]$ (**4**), $[PPh_4]_2[Ru_6C(CO)_{14}(SO_2)_2]$ (**6**), and $[PPN][Ru_6C(CO)_{15}(SO_2Me)]$ (**7**)

	2	**4**·C_2H_5OH	**6**	**7**
chem formula	$C_{17}O_{18}Ru_6S$	$C_{82}H_{60}N_2O_{17}P_4Ru_6S\cdot C_2H_5OH$	$C_{63}H_{40}O_{18}P_2Ru_6S_2$	$C_{53}H_{33}NO_{17}P_2Ru_6S$
a, Å	18.232(4)	24.849(2)	25.517(3)	34.331(4)
b, Å	9.328(1)	14.616(1)	14.064(5)	10.280(2)
c, Å	17.442(4)	24.612(2)	20.008(2)	16.415(2)
α, deg	90	90	90	90
β, deg	115.884(9)	92.078(6)	111.391(9)	94.85(1)
γ, deg	90	90	90	90
V, Å^3	2668.6(9)	8933.1(13)	6686(2)	5772(1)
Z	4	4	4	4
fw	1130.66	2179.82 + 46.07	1817.49	1656.27
space group (No.)	$P2_1/a$ (14)	$P2_1/c$ (14)	$P2_1/a$ (14)	$P2_1/n$ (14)
T, °C	21	21	21	21
λ, Å	0.710 73	0.710 73	0.710 73	0.710 73
ρ_{calcd}, g cm^{-3}	2.67	1.65	1.81	1.91
μ, cm^{-1}	33.90	11.29	14.70	16.58
$R(F_o)^a$	0.0242	0.0447	0.0412	0.0358
$R_w(F_o)^b$	0.0254	0.0472	0.0380	0.0264

^{a} $R = \sum||F_o| - |F_c||/\sum|F_o|$. ^{b} $R_w = [\sum w(|F_o| - |F_c|)^2/\sum w|F_o|^2]^{1/2}$.

up by alumina column chromatography (5% water, 1.8 cm internal diameter × 20 cm). A red band which was eluted with CH_2Cl_2 was collected and evaporated to dryness. Recrystallization of the residue from CH_2Cl_2−methanol gave red-brown crystals (56 mg, 55%) (Found: C, 39.17; H, 2.09; N, 0.86. Calcd for $C_{54}H_{35}NO_{16}P_2Ru_6S$: C, 39.21; H, 2.13; N, 0.85). IR: (cm^{-1}): *ν*(CO) (CH_2Cl_2) 2066 m, 2024 w (sh), 2015 vs, and 1961 w; *ν*(SO) (KBr) 1218 m and 1062 s. ^{1}H NMR ($CDCl_3$) 0.37 (d, 2H, J = 12.2 Hz, *anti*-H), 1.55 (1H, tt, J = 12.2 and 7.2 Hz, *central*-H), 3.83 (2H, d, J = 7.2 Hz, *syn*-H), 7.68−7.39 (30H, m, C_6H_5).

Synthesis of [PPN][Ru$_6$C(CO)$_{14}$(NO)(SO$_2$)] (13). Through a solution of **4** (100 mg, 0.046 mmol) in CH_2Cl_2 (20 cm^3) was bubbled NO for 5 min (one bubble/s) with stirring, giving an immediate color change from red to red-brown. The solvent was removed from the resulting solution under reduced pressure, and the residue taken up in CH_2Cl_2 and chromatographed on silica gel column (1.8 cm internal diameter × 25 cm). Elution with CH_2Cl_2−ethyl acetate (4:1 v/v) separated a red band. Evaporation of the eluate to dryness afforded red crystals, which is recrystallized from CH_2Cl_2−hexane (26 mg, 34%) (Found: C, 37.39; H, 1.86; N, 1.80. Calcd for $C_{51}H_{30}N_2O_{17}P_2Ru_6S$: C, 37.28; H, 1.84; N, 1.70). IR (cm^{-1}): *ν*(CO) (CH_2Cl_2) 2074 m, 2033 vs, 2017 w (sh), 1979 w, and 1827 w; *ν*(NO) (CH_2Cl_2) 1751 w; *ν*(SO) (KBr) 1231m and 1068s.

Structure Determination. Deep red single crystals of **2** were obtained by recrystallization from hot THF solution. Red single crystals of **4** were grown by diffusion of hexane into the ethanol solution in a glass tube (internal diameter 8 mm). Due to the large number of non-hydrogen atoms to be located and refined in $[PPN]^+$ salt, a crystal structure determination of **5** was not carried out on this material and the $[PPh_4]^+$ salt was prepared. Single crystals of $[PPh_4]_2[Ru_6C(CO)_{14}(SO_2)_2]$ (**6**) suitable for X-ray analysis were obtained by slow diffusion of hexane into an ethanol solution of the compound. Dark red single crystals of **7** were obtained by cooling of a CH_2Cl_2−methanol solution to −20 °C. Deep green single crystals of **8** were obtained by addition of hexane to a CH_2Cl_2 solution in flask at room temperature. Due to disorder problems a crystal structure determination of **10** was not successful, so the $[PPh_4]^+$ salt of the cluster anion was prepared. Single crystals of $[PPh_4][Ru_6C(CO)_{14}(C_3H_5)(SO_2)]$ (**11**) suitable for X-ray analysis were obtained by slow diffusion of hexane into an ethanol solution of the compound in a glass tube. Red crystals of **13** were grown by diffusion of hexane into the CH_2Cl_2 solution in a flask at ambient temperature. All the single crystals were fixed with Apiezon grease L in a glass capillaries under argon. Intense data were collected by use of an Enraf-Nonius CAD4 four-circle automated diffractometer with graphite-monochromated Mo Kα radiation. Crystal data and experimental details are given in Tables 8 and 9.

A survey of the data set for complex **2** and the systematic extinction indicated the centrosymmetric monoclinic space group $P2_1/a$. Data were corrected for absorption.[49] The analytical form of the scattering factor[50] for the appropriate neutral atom was corrected for both real

Table 9. Crystallographic Data for $Ru_6C(CO)_{15}(SO)$ (**8**), $[PPh_4][Ru_6C(CO)_{14}(C_3H_5)(SO_2)]$ (**11**), and $[PPN][Ru_6C(CO)_{14}(NO)(SO_2)]$ (**13**)

	8	**11**	**13**
chem formula	$C_{16}O_{16}Ru_6S$	$C_{42}H_{25}O_{16}PRu_6S$	$C_{51}H_{30}N_2O_{17}P_2Ru_6S$
a, Å	16.834(3)	32.505(7)	14.937(4)
b, Å	9.644(4)	18.764(2)	18.071(5)
c, Å	33.800(7)	15.929(3)	10.615(3)
α, deg	90	90	102.45(1)
β, deg	107.454(8)	100.332(9)	93.16(2)
γ, deg	90	90	79.20(2)
V, Å^3	5234(2)	9558(3)	2747.8(12)
Z	8	8	2
fw	1086.65	1455.10	1643.23
space group (No.)	*Cc* (9)	$P2_1/n$ (14)	$P\bar{1}$ (2)
T, °C	21	21	21
λ, Å	0.710 73	0.710 73	0.710 73
ρ_{calcd}, g cm^{-3}	2.76	2.02	1.99
μ, cm^{-1}	34.63	19.55	17.41
$R(F_o)^a$	0.0516	0.0797	0.0352
$R_w(F_o)^b$	0.0496	0.0665	0.0342

^{a} $R = \sum||F_o| - |F_c||/\sum|F_o|$. ^{b} $R_w = [\sum w(|F_o| - |F_c|)^2/\sum w|F_o|^2]^{1/2}$.

($\Delta f'$) and imaginary ($\Delta f''$) components of anomalous dispersions.[51] The structure was solved by direct methods MULTAN,[52] which located six ruthenium atoms. All the remaining atoms were located from subsequent Fourier-difference syntheses. They were refined by the block-diagonal least-squares method[53] with anisotropic thermal parameters for all atoms. The final $R(F)$ and $R_w(F)$ values converged to 0.024 and 0.025 with the weighting scheme $w = 1$. The final Fourier-difference synthesis showed no unexpected features, with the highest peak 0.60 e Å^{-3} within the covalent radius of the ruthenium atom (0.78 Å from Ru(2)).

A survey of the data set for complex **4** and the systematic extinction indicated the centrosymmetric monoclinic space group $P2_1/c$. The structure was solved and refined as for **2**. The hydrogen atoms in the phenyl groups of the countercation were not located. All the non-hydrogen atoms were refined with anisotropic thermal parameters.

(49) North, A. C. T.; Phillips, D. C.; Mathews, F. S. *Acta Crystallogr.* **1968**, *A24*, 351.
(50) Cromer, D. T.; Waber, J. T. *International Tables for X-Ray Crystallography*; Ibers, J. A., Hamilton, W. C., Eds.; Kynoch Press: Birmingham, U.K., 1974; Vol. IV, p 71.
(51) Cromer, D. T. *International Tables for X-Ray Crystallography*; Ibers, J. A., Hamilton, W. C., Eds.; Kynoch Press: Birmingham, U.K., 1974; Vol. IV, p 148.
(52) Main, P.; Hull, S. E.; Lessinger, L.; Germain, G.; Declerq, J.-P.; Woolfson, M. M. MULTAN 78; University of York: York, England, 1978.
(53) Sakurai, T.; Kobayashi, K. *Rikagaku Kenkyusho Hokoku* **1979**, *55*, 69.

Cluster **4** crystallized with a molecule of ethanol in the asymmetric crystal unit, which were refined isotropically. The final $R(F)$ and $R_w(F)$ values are 0.045 and 0.047 with the weighting scheme $w = 1$.

A survey of the data set for complex **6** and the systematic extinction indicated the centrosymmetric monoclinic space group $P2_1/a$. The structure was solved and refined as for **2**. All the non-hydrogen atoms were treated with anisotropic thermal parameters. As refinement proceeded all the remaining hydrogen atoms in the phenyl groups of the countercations were located from subsequent Fourier-difference syntheses, and refined with isotropic thermal parameters. The final $R(F)$ and $R_w(F)$ values converged to 0.024 and 0.025 with the weighting scheme $w = 1/\sigma^2(F_o)$.

A survey of the data set for complex **7** and the systematic extinction indicated the centrosymmetric monoclinic space group $P2_1/n$. The structure was solved and refined as for **2**. Three hydrogen atoms in the methyl group of the cluster anion were located from subsequent Fourier-difference syntheses. All non-hydrogen atoms were refined with anisotropic thermal parameters, and the methyl hydrogen atoms were refined with an isotropic thermal parameter. As refinement proceeded, the hydrogen atoms in the phenyl groups of the countercation were added in their idealized positions for the structure factor calculations, but their positions were not refined. The final model converged to $R(F)$ 0.036 and $R_w(F)$ 0.026 with the weighting scheme $w = 1/\sigma^2(F_o)$.

A survey of the data set for complex **8** and the systematic extinction indicated the centrosymmetric monoclinic space group $C2/c$ or non-centrosymmetric monoclinic space group Cc. The former possibility was indicated by the cell volume (consistent with $Z = 8$), but successful refinement of the structure was obtained by the latter lower-symmetry space group in which two crystallographically independent clusters were contained. The structure was solved and refined as for **2**. All the non-hydrogen atoms were treated with anisotropic thermal parameters. At the final stage subsequent Fourier-difference map revealed six high peaks (4.5−5.5 e/Å^3) more than 1.0 Å apart from Ru(1B)−Ru(6B). The six peaks are 2.8−4.1 Å apart from each other locating about 2.0 Å from the carbide atom C(0B) and constitute an octahedron. Hence, the peaks were assigned as ruthenium atoms of a disordered molecule of the second cluster **8**; however, it was not located because of their low electron densities. The next higher peak with 1.28 e Å^{-3} by the Fourier-difference synthesis showed no unexpected features. The final $R(F)$ and $R_w(F)$ values are 0.052 and 0.050 with the weighting scheme $w = 1/\sigma(F_o)$.

A survey of the data set for complex **11** and the systematic extinction indicated the centrosymmetric monoclinic space group $P2_1/n$. The structure was solved and refined as for **2**. The hydrogen atoms were not located. All the non-hydrogen atoms were refined with anisotropic thermal parameters. The final $R(F)$ and $R_w(F)$ values were 0.080 and 0.067 with the weighting scheme $w = 1/\sigma^2(F_o)$. The unit cell contains chemically equivalent two independent cluster anions and counter cations.

A survey of the data set for complex **13** revealed no systematic extinctions and no symmetry other than the Friedel condition ($\bar{1}$). Thus, the crystal belongs to the triclinic class with space group $P1$ or $P\bar{1}$. The latter centrosymmetric possibility was strongly indicated by the cell volume (consistent with $Z = 2$) and was confirmed by the successful refinement of the structure. The structure was solved and refined as for **2**. All the non-hydrogen atoms were treated with anisotropic thermal parameters. As refinement proceeded, all the remaining hydrogen atoms in the phenyl groups of the countercations were located from subsequent Fourier-difference syntheses and refined with isotropic thermal parameter. Assignment of the NO ligand was made by the short bond length to the ruthenium atom compared with that of CO. Replacement of the nitrogen atom by a carbon atom led to marginally higher residual and GOF values, indicating that the determination was correct. The final $R(F)$ and $R_w(F)$ values are 0.035 and 0.034 with the weighting scheme $w = 1$.

Supporting Information Available: For complexes **2**, **4**, **6**−**8**, **11**, and **13**, tables listing full atomic coordinates, equivalent isotropic and anisotropic temperature factors, and bond lengths and bond angles (28 pages). Ordering information is given on any current masthead page.

IC9704290